Journal of Research in Pharmacy
Research Article
www.jrespharm.com

Synthesis and *in vitro* anticancer activity of some new hydrazide-hydrazones derived from articaine

Sevgi KARAKUŞ [1] *, Fatih TOK [2], Burçin İrem ABAS [3], Elif TÜTÜNCÜ [2], Nigar Kübra KALKAN [2], Sevda TÜRK [4], Özge ÇEVİK [3]

1 Department of Pharmaceutical Chemistry, Faculty of Pharmacy, İstanbul Aydın University, 34295 İstanbul, Türkiye.
2 Department of Pharmaceutical Chemistry, Faculty of Pharmacy, Marmara University, 34854 İstanbul, Türkiye.
3 Department of Biochemistry, School of Medicine, Aydın Adnan Menderes University, 09010 Aydın, Türkiye.
4 Department of Pharmaceutical Chemistry, Faculty of Pharmacy, Karadeniz Technical University, 61000 Trabzon, Türkiye.

* Corresponding Author. E-mail: sevgikarakus@aydin.edu.tr (S.K.); Tel. 444-1-428.

Received: 2 August 2024 / Revised: 1 September 2024 / Accepted: 1 September 2024

ABSTRACT: In this study, synthesis of some new hydrazone derivatives based on articaine was carried out. MDA-MB-231 (triple negative human breast cancer cells) and HUVEC (human umbilical vein endothelial cells) cells were used to investigate the cytotoxic activity of hydrazone compounds. Induction of apoptosis and cell viability were assessed by AnnexinV-PI binding levels and Bax-Bcl2 gene expression levels. Inhibitory activities of the compounds against carbonic anhydrase enzyme were also evaluated. Compounds **2b** and **2m** exhibited the highest cytotoxic activity against MDA-MB-231 cells with IC_{50} values of 16.62±1.18 µM and 18.56±2.36 µM, respectively. Similarly, the CA inhibition of **2b** and **2m** was also determined to be the highest in the series.

KEYWORDS: Hydrazone; Articaine; breast cancer; carbonic anhydrase; bax.

1. INTRODUCTION

Breast cancer is the most common type of cancer and is also the leading cause of cancer-related deaths in women worldwide [1]. The World Health Organisation (WHO) reported 3.0 million cases of breast cancer out of a total of 20 million new cancer cases in 2022, and predicts that the total number of new cancer cases will reach 31 million and breast cancer cases will reach 3.1 million in 2045 [2]. Different methods are preferred to treat breast cancer. Treatment with chemotherapeutics with antiestrogenic effect or surgical removal of the breast are important alternative methods to prevent breast cancer [3]. In the treatment of patients diagnosed with breast cancer, there are different treatment strategies such as targeted therapy, hormonal therapy, radiotherapy, surgery and chemotherapy [4]. However, difficulties such as side effects during treatment, the strong resistance of breast cancer to treatment and cost encourage scientists to find different alternative methods [5].

Hydrazide-hydrazone is one of the most common groups in the development of new drug candidates in medicinal chemistry [6, 7]. Different biological activities such as antimicrobial, antidepressant, antidiabetic, anticancer, anti-inflammatory, antidiabetic, anticancer, anti-inflammatory by interacting with different enzymes and receptors are the reasons for the preference of hydrazide-hydrazones [8-10]. There are many literature showing the activity of hydrazide-hydrazone groups against various types of cancer [11]. Acar-Çevik et al. reported that the benzimidazole-hydrazone derivatives they synthesized showed higher cytotoxic activity than cisplatin against MCF-7 breast cancer cells [12]. Osmaniye et al. reported that benzothiazole-acylhydrazone derivatives synthesized by them showed significant cytotoxic effects against MCF7 as well as C6, A549, HT29 cancer cells [13]. In addition, different hydrazone structures with anticancer activity have been shown in our previous studies [14-16].

Based on the literature data, synthesis of some new hydrazide-hydrazone derivatives from articaine compound has been carried out in this study. The cytotoxic activities of the synthesized compounds against MDA-MB-231 (triple negative human breast cancer cells) and HUVEC (human umbilical vein endothelial

How to cite this article: Karakus S, Tok F, Abas BI, Tutuncu E, Kalkan NK, Turk S, Cevik O. Synthesis and in vitro anticancer activity of some new hydrazide-hydrazones derived from articaine. J Res Pharm. 2024; 28(6): 1901-1910.

ISSN: 2630-6344
http://dx.doi.org/10.29228/jrp.863

cells) were determined by MTT method. Additionally, the activity of the compounds against the carbonic anhydrase enzyme inhibition and Hif1a (hypoxia-inducible factor-1 alpha) were examined.

2. RESULTS

2.1. Chemistry

The hydrazide-hydrazones, target compounds were synthesized in two steps, starting from articaine. In the first step, the ester group in the articaine molecule was treated with hydrazine monohydrate in ethanol medium to obtain the hydrazide compound (**1**). Then, the hydrazide compound (**1**) was reacted with various aldehyde derivatives and the target compounds, hydrazide-hydrazone derivatives (**2a-2m**), were synthesized (**Scheme 1**). The structures of the synthesized compounds were elucidated by IR, ^{1}H-NMR and ^{13}C-NMR spectra.

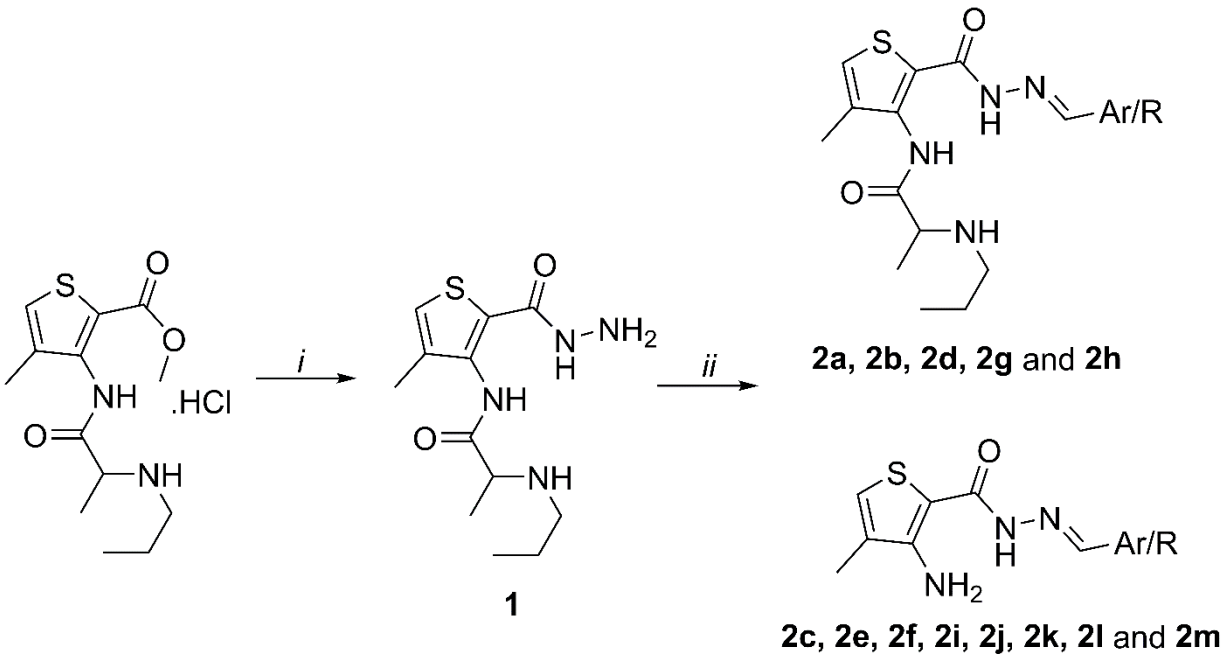

Scheme 1. The synthesis pathway of hydrazide-hydrazones (**2a-2m**). Reagents and conditions: (i) hydrazine monohydrate, EtOH, reflux for 4 h. (ii) Substituted aldehydes and EtOH, reflux for 6-8 h.

Interestingly, two different groups of compounds were obtained during hydrazone synthesis, although under the same conditions. During the synthesis of compounds **2a**, **2b**, **2d**, **2g** and **2h**, the overall structure of the articaine molecule was preserved, whereas during the synthesis of compounds **2c**, **2e**, **2f**, **2i**, **2j**, **2k**, **2l** and **2m**, the amide group on the thiophene ring was hydrolyzed. In the IR spectra of the hydrazone structure, imine (C=N) and N-H bonds were detected in the range of 1573-1624 cm^{-1} and 3228-3535 cm^{-1}, respectively. In the ^{1}H-NMR spectra of the compounds, N-H protons were recorded between 11.15 ppm and 11.54 ppm. The NH protons of compounds **2d** and **2l** could not be detected in the ^{1}H-NMR spectra because they were replaced by deuterium.

2.2. Biological activity

The MDA-MB-231 (human breast cancer cells), HUVEC (human umbilical vein endothelial cells) were used to examine the cytotoxic activities of the synthesized compounds. In addition, the activities of the compounds against the carbonic anhydrase enzyme were evaluated and the data are presented in **Table 1**.

Table 1. The anticancer activity results of hydrazide-hydrazones (**2a-2m**).

Compounds	MDA-MB-231 (IC_{50}, µM)	HUVEC (IC_{50}, µM)	Selective Index (HUVEC/MDA-MB-231)	CA inhibition % (10 µM)
2a	93,05±2,63	102,05±4,14	1,10	2,14±1,05
2b	16,62±1,18	168,63±2,05	10,15	51,02±3,41
2c	139,03±3,69	122,07±7,63	0,88	4,62±1,06
2d	175,02±4,16	164,10±6,21	0,94	22,04±1,08
2e	61,94±5,30	72,92±6,04	1,18	15,03±2,36
2f	66,05±5,36	77,02±5,32	1,17	11,04±2,07
2g	58,42±4,79	42,14±4,86	0,72	8,06±3,34
2h	239,06±5,66	187,96±2,08	0,79	7,09±1,21
2i	279,03±2,87	297,63±5,11	1,07	5,65±1,32
2j	232,84±4,63	255,47±7,42	1,10	26,18±5,66
2k	203,33±6,97	226,83±3,39	1,12	30,05±3,40
2l	171,64±4,58	115,06±5,06	0,67	17,06±3,62
2m	18,56±2,36	93,05±4,17	5,01	43,05±5,43
Acetazolamide	47,12±4,28	53,07±6,03	1,13	9,11±3,45

The morphology and cell viability of compounds were evaluated with MDA-MB-231 cells at 10 µM concentrations after incubation for 24 and 48 hours. It was determined that the compounds had decreased interaction with each other and their growth slowed down compared to the control group in morphological changes in the cells (**Figure 1**). While a decrease in cell viability was observed in compounds **2a**, **2b, 2i, 2f** at 24 hours of incubation, a decrease was observed in compounds **2b**, **2f**, **2g**, **2l**, **2m** at 48 hours of incubation. According to both cell viability and selective index of the cells, compounds that were effective on cancer cells but had no effect on healthy cells were selected from the compounds that were effective at the lowest concentrations. The four compounds that were effective according to SI values were determined as compounds **2b, 2m, 2e** and **2f**, respectively (**Table 1**). When the carbonic anhydrase inhibition values of the compounds were examined at 10 µM concentration, the four effective compounds were seen as **2b, 2m, 2k,** and **2j** respectively. When these evaluations were taken together, compounds **2b** and 2**m,** which showed low dose effects in both SI and CA inhibition, were determined as anti-cancer candidate compounds.

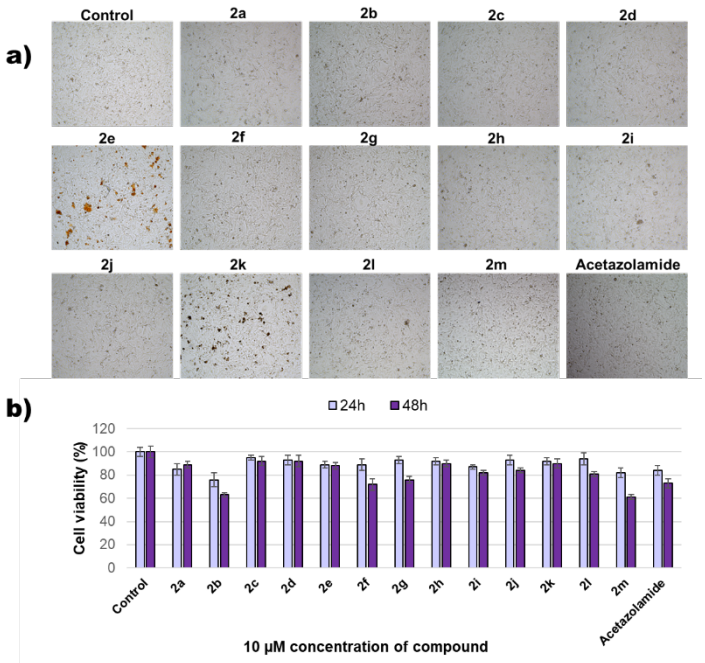

Figure 1. Morphology and cell viability of 10 µM compounds in MDA-MB-231 cells.

MDA-MB-231 cells are triple negative breast cancer cells. It is known that CA expression is high in these cells [17]. CAIX levels can be particularly high in breast cancer and inhibitors are used for this. It is known that the levels of this enzyme are also high in hypoxic conditions. Cancer cells can exhibit a more

resistant mechanism by creating a hypoxic environment and this is important in drug resistance. Since cancer cells can survive in more acidic environments, they can change their mechanisms against some treatments. Hif1a is a protein that increases in hypoxic conditions and allows cells to survive at low pH levels, and especially strengthens hypoxic adaptation in the tumor [18]. It is known that there is a relationship between CA and Hif1a, and since CA can control hydrogen flux, when its levels increase in hypoxic environments, the expression of proteins such as Hif1a in the cell may also increase [19]. We found that the compounds we synthesized, **2b** and **2m**, decreased both the gene and protein levels of Hif1a, and this decrease was statistically significant (p<0,001) (**Figure 2**).

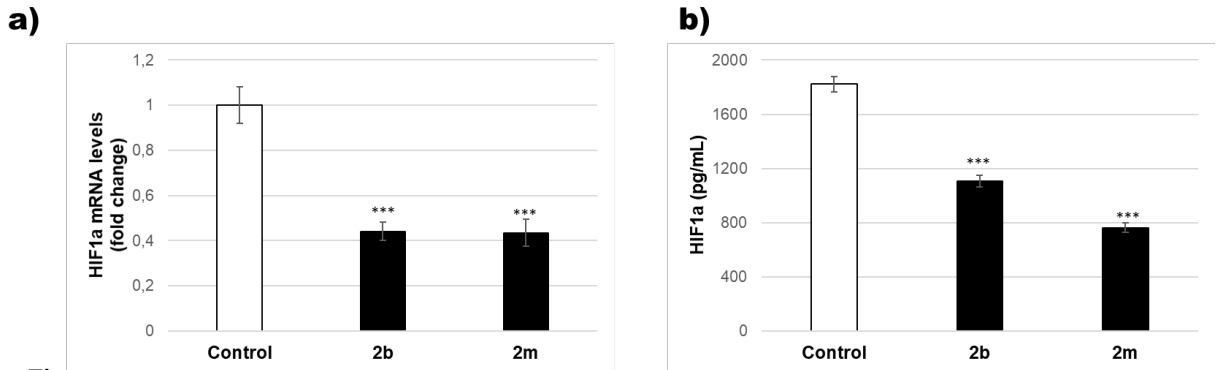

Figure 2. Hif1a gene and protein expression of compound **2b** and **2m** in MDA-MB-231 cells.

AnnexinV-PI binding is also an indicator of apoptosis. Phosphatidylserine, which is located on the inner surface of the cell membrane, goes outside the cell membrane when apoptotic signals start in the cell and annexin-V binds to it. PI is a dye that binds to DNA, and its binding increases in late apoptosis and necrosis. Apoptosis rates are determined by looking at the binding of these dyes together. We counted the early apoptosis and late apoptosis MDA-MB-231 cells with flow cytometry after incubation with **2b** and **2m** compounds and calculated the total apoptosis value (**Figure 3**). In **2b** and **2m** compounds, total apoptotic cells increased more than 20 fold compared to control group cells and this increase was found to be significant in both compounds (p<0,001).

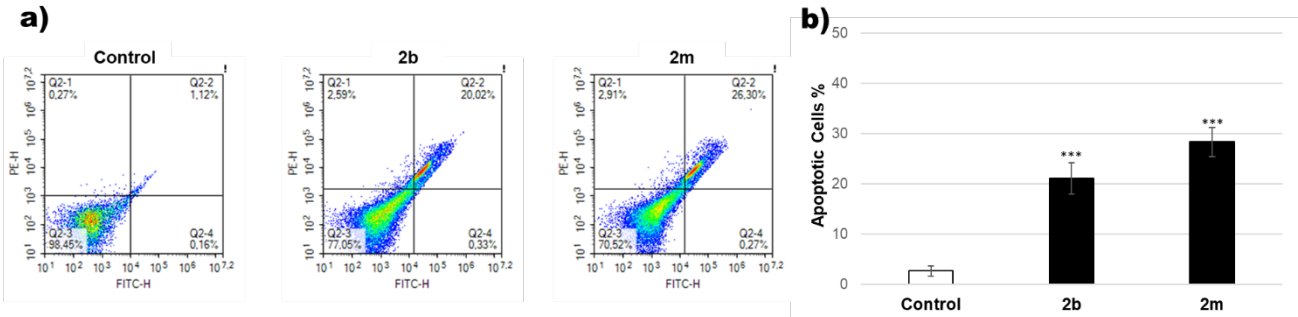

Figure 3. Annexin-V and PI binding levels of compound **2b** and **2m** in MDA-MB-231 cells.

JC-1 is an important marker showing mitochondrial changes. When the cell goes to apoptosis through the internal pathway, the mitochondrial membrane potential changes. The dye is bicolored. The red color shows the aggregate form of undamaged mitochondria. The green one is the monomer, it indicates that there is a change in the mitochondrial membrane and some proteins have started to be released. When we looked at the change in both stainings in flow cytometry and took their ratios, we counted them after incubation with **2b** and **2m** compounds in MDA-MB-231 cells and calculated the mitochondrial membrane change value (**Figure 4**). In **2b** and **2m** compounds, the red/green ratio decreased by almost 3 times compared to the control group cells, and this increase was found to be significant in both compounds (p<0,001).

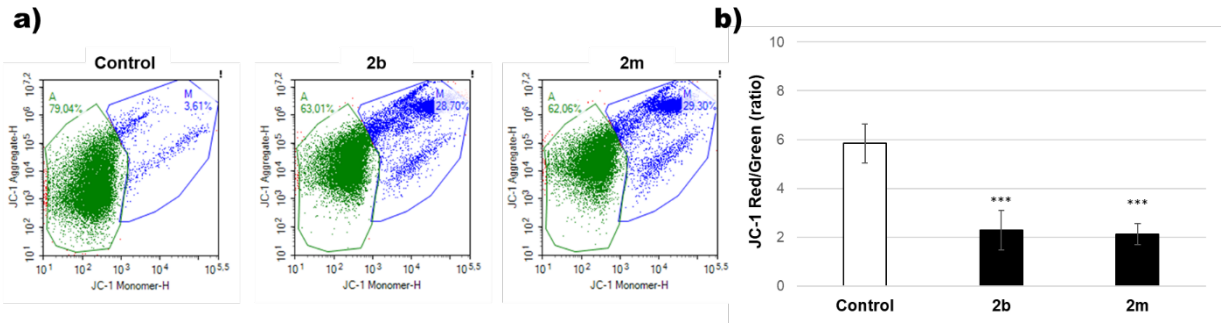

Figure 4. JC-1 monomer and aggregate levels of compound **2b** and **2m** in MDA-MB-231 cells.

Bax and Bcl-2 are two basic proteins involved in apoptosis. Bax is pro-apoptotic and Bcl-2 is anti-apoptotic. Their ratio in the cell is important and when we evaluated the Bax/Bcl-2 ratios together, we measured the effect of the candidate compounds. When we looked at the Bax/Bcl-2 ratio, we found that the **2b and 2m** compounds were effective on mitochondrial apoptosis in the cell (**Figure 5**). Bax gene expression increased significantly in compound **2m** ($p<0,001$), but did not show a significant increase in compound **2b** (**Figure 5a**). Bcl2 gene expression decreased significantly in compound **2b** and **2m**, and this decrease was greater in compound **2m** (**Figure 5b**, $p<0,001$). The Bax/Bcl-2 ratio increased 1.5 times in the **2b** compound compared to the control group, while it increased 4 times in the **2m** compound (**Figure 5c**, $p<0,001$).

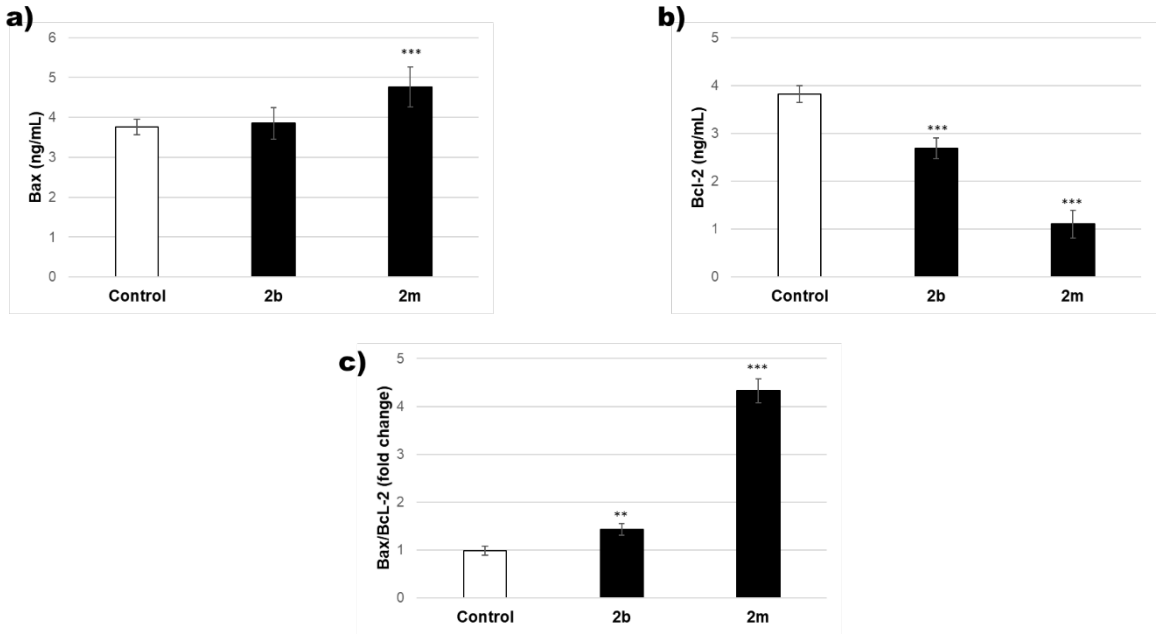

Figure 5. Bax and Bcl-2 gene expression levels of compound **2b** and **2m** in MDA-MB-231 cells.

3. CONCLUSION

Breast cancer is one of the cancers with the highest mortality rate. Based on the strong anticancer effects of hydrazide-hydrazone derivatives, some new hydrazone derivatives were synthesized in this study. The cytotoxic activities of the compounds were evaluated on MDA-MB-231 cells. In addition, MTT assay was performed on HUVEC cells to determine the selectivity indices of the compounds. CA inhibition and Hif1a suppression offer new approaches in triple negative breast cancer treatments. Drug designs that can affect the behavior of cancer cells living in hypoxic conditions have gained importance in recent years. In this study, compounds **2b** and **2m** provided CA inhibition, suppressing Hif1a at both gene and protein levels, reducing cell viability and accelerating apoptosis. Compounds **2b** and **2m** may be a new anticancer candidate by inhibiting the CA enzyme for non-toxic long-term treatments for triple negative breast cancer.

4. MATERIALS AND METHODS

4.1. Chemistry

4.1.1. General procedure for the synthesis of compounds (2a-m).

The compounds (2a-m) were synthesized via the method in our previous papers [14-16].

N-(2-(2-(4-(Trifluoromethyl)benzylidene)hydrazine-1-carbonyl)-4-methylthiophen-3-yl)-2-(propylamino)propanamide **(2a)** White solid, yield: 75%, mp: 156 °C. FT-IR: υmax (cm^{-1}): 3255 (NH) 2974 (=CH) 2931, 2862, 2829 (CH), 1696 (C=O), 1620 (C=N), 1122 (C-F). ^{1}H NMR (400 MHz, DMSO-d_6) δ 0.82 (3H, t, $CH_2CH_2\underline{CH_3}$), 1.63 (3H, d, $COCH\underline{CH_3}$), 1.44 (2H, m, $CH_2\underline{CH_2}CH_3$), 2.29 (3H, s, thiophene-CH_3), 2.68 (2H, t, $\underline{CH_2}CH_2CH_3$), 3.97(1H, s, $\underline{NH}CH_2CH_2CH_3$), 5.07 (1H, m, $CO\underline{CH}CH_3$), 6.90 (1H, s, Ar-H), 7.60-8.10 (5H, m, hydrazone CH and Ar-H), 11.44 (1H, s, hydrazone NH). ^{13}C NMR (100 MHz, DMSO-d_6) δ 11.88, 13.02, 20.25, 55.82, 76.55, 21.01, 119.9, 123.28, 125.52, 125.98, 126.27, 127.87, 128.65, 129.97, 130.36, 133.53, 139.12, 145.60, 154.59,156.17. MS (ES m/z): 462 (M^+-H+Na), 453, 435, 421, 417.

N-(2-(2-(2-Hydroxy-3-methoxybenzylidene)hydrazine-1-carbonyl)-4-methylthiophen-3-yl)-2-(propylamino)propanamide **(2b)** Cream solid, yield: 65%, mp: 180-183 °C. FT-IR: υmax (cm^{-1}): 3545 (OH), 3352 (NH), 3130 (=CH), 2958 (CH), 1635 (C=O), 1606 (C=N). ^{1}H NMR (400 MHz, DMSO-d_6) δ 2.01 (3H, s, thiophene-CH_3), 3.79 (3H, s, OCH_3), 6.86 (1H, s, Ar-H), 7.46-8.33 (4H, m, hydrazone CH and Ar-H), 9.41 (1H, s, OH), 11.28 (1H, s, hydrazone NH). ^{13}C NMR (100 MHz, DMSO-d_6) δ 13.05, 56.29, 56.33, 61.17, 105.44, 112.51, 114.40, 118.56, 119.04, 119.24, 119.50, 122.39, 125.22, 127.59, 131.14, 144.14, 147.73, 148.23, 148.41, 148.68, 151.15, 158.16. MS (ES m/z): 438 (M^++H+K), 415, 304, 141, 59.

3-Amino-4-methyl-*N*'-(4-nitrobenzylidene)thiophene-2-carbohydrazide **(2c)** Red solid, yield: 65%, mp: 278 °C. FT-IR: υmax (cm^{-1}): 3404 (NH) 3037 (=CH) 2964, 2929, 2850 (CH), 1622 (C=O), 1384 (NO_2). ^{1}H NMR (400 MHz, DMSO-d6) δ 2.05 (3H, s, thiophene-CH3), 6.92 (1H, s, Ar-H), 7.34-8.17 (5H, m, hydrazone CH and Ar-H), 11.54 (1H, s, hydrazone NH). ^{13}C NMR (100 MHz, DMSO-d_6) δ 13.35, 124.64, 128.18, 141.55, 147.81.

N-(2-(2-(4-Nitrobenzylidene)hydrazine-1-carbonyl)-4-methylthiophen-3-yl)-2-(propylamino)propanamide **(2d)** White solid, yield: 75%, mp: 156 °C. FT-IR: υmax (cm^{-1}): 3250 (NH), 2968 (=CH), 2868, 2827 (CH), 1654 (C=O), 1575(C=N), 1340 (NO_2). ^{1}H NMR (400 MHz, DMSO-d_6) δ 0.83 (3H, t, $CH_2CH_2\underline{CH_3}$), 1.63 (3H, d, $COCH\underline{CH_3}$), 1.45 (2H, m, $CH_2\underline{CH_2}CH_3$), 2.28 (3H, s, thiophene-CH_3), 2.68 (2H, t, $\underline{CH_2}CH_2CH_3$), 3.97 (1H, s, $\underline{NH}CH_2CH_2CH_3$), 5.14 (1H, m, $CO\underline{CH}CH_3$), 7.70-8.20 (6H, m, hydrazone CH and Ar-H). ^{13}C NMR (100 MHz, DMSO-d_6) δ 12.01, 12.97, 19.89, 21.02, 55.84, 56.49, 76.25, 119.95, 123.70, 129.65, 130.55, 133.85, 147.81, 147.97, 154.20, 154.58, 156.10. MS (ES m/z): 417 (M^+), 414, 412, 398, 389.

3-Amino-4-methyl-*N*'-(pyridin-4-ylmethylidene)thiophene-2-carbohydrazide **(2e)** Yellow solid, yield: 75%, mp: 244 °C. FT-IR: υmax (cm^{-1}): 3292 (NH), 3030 (=CH), 2929, 2850 (CH), 1606 (C=O). ^{1}H NMR (400 MHz, DMSO-d_6) δ 2.04 (3H, s, thiophene-CH_3), 6.92 (1H, s, Ar-H), 7.69-8.66 (5H, m, hydrazone CH and Ar-H), 11.51 (1H, s, hydrazone NH). ^{13}C NMR (100 MHz, DMSO-d_6) δ 13.35, 96.91, 121.29, 127.49, 139.68, 142.27, 150.72, 156.73, 165.44. MS (ES m/z): 259 (M^+-H), 113.

3-Amino-4-methyl-*N*'-(4-methoxybenzylidene)thiophene-2-carbohydrazide **(2f)** Yellow solid, yield: 75%, mp: 174-177 °C. FT-IR: υmax (cm^{-1}): 3462 (NH), 3136 (=CH), 2933, 2835 (CH), 1624 (C=O), 1585 (C=N). ^{1}H NMR (400 MHz, DMSO-d_6) δ 0.82 (3H, t, $CH_2CH_2\underline{CH_3}$), (3H, d, $COCH\underline{CH_3}$), 1.06 (2H, m, $CH_2\underline{CH_2}CH_3$), 2.09 (3H, s, thiophene-CH_3), 2.68 (2H, t, $\underline{CH_2}CH_2CH_3$), 3.97 (1H, s, $\underline{NH}CH_2CH_2CH_3$), 5.07 (1H, m, $CO\underline{CH}CH_3$), 7.02 (1H, s, Ar-H), 7.69-7.96 (5H, m, hydrazone-CH and Ar-H), 11.20 (1H, s, hydrazone NH). ^{13}C NMR (100 MHz, DMSO-d_6) δ 13.37, 55.72, 97.57, 114.84, 127.41, 127.74, 128.93, 130.57, 142.00, 156.10, 160.81, 165.43. MS (ES m/z): 288 (M^+-H), 198, 113.

N-(2-(2-(Thiophen-2-ylmethylene)hydrazine-1-carbonyl)-4-methylthiophen-3-yl)-2-(propylamino)propanamide **(2g)** Grey solid, yield: 60%, mp: 108 °C. FT-IR: υmax (cm^{-1}): 3238 (NH), 2964 (=CH), 2964, 2936, 2349 (CH), 1696 (C=O), 1620 (C=N). ^{1}H NMR (400 MHz, DMSO-d_6) δ 0.82 (3H, t, $CH_2CH_2\underline{CH_3}$), 1.63 (3H, d, $COCH\underline{CH_3}$), 1.44 (2H, m, $CH_2\underline{CH_2}CH_3$), 2.29 (3H, s, thiophene-CH_3), 2.68

(2H, t, $\underline{CH_2}CH_2CH_3$), 3.97 (1H, s, $\underline{NH}CH_2CH_2CH_3$), 5.07 (1H, m, CO$\underline{CH}CH_3$), 6.90 (1H, s, Ar-H), 7.60-8.10 (5H, m, hydrazone CH and Ar-H), 11.44 (1H, s, hydrazone NH). ^{13}C NMR (100 MHz, DMSO-d_6) δ 12.14, 12.93, 18.49, 21.30, 56.04, 56.31, 72.87, 119.46, 124.81, 125.82, 126.36, 127.02, 127.67, 127.94, 130.25, 133.83, 146.35, 154.14, 154.49, 154.96.

N-(2-(2-(4-Hydroxybenzylidene)hydrazine-1-carbonyl)-4-methylthiophen-3-yl)-2-(propylamino)propanamide **(2h)** Cream solid, yield: 60%, mp: 176 °C. FT-IR: υmax (cm^{-1}): 3734 (OH), 3535 (NH), 2960 (=CH), 2935, 2874, 2349 (CH), 1681 (C=O), 1624 (C=N). ^{1}H NMR (400 MHz, DMSO-d_6) δ 2.01 (3H, s, thiophene-CH_3), 3.79 (3H, s, OCH_3), 6.86 (1H, s, Ar-H), 7.46-8.33 (4H, m, hydrazone CH and Ar-H), 9.41 (1H, s, OH), 11.28 (hydrazone NH). ^{13}C NMR (100 MHz, DMSO-d_6) δ 11.88 ($CH_2CH_2\underline{CH_3}$), 13.02 (thiophene-CH_3), 20.25 (COCH$\underline{CH_3}$), 55.82 ($\underline{CH_2}CH_2CH_3$), 76.55 (CO$\underline{CH}CH_3$), 21.01 ($CH_2\underline{CH_2}CH_3$), 119.9, 123.28, 125.52, 126.27, 127.87, 129.97, 130.36, 133.53, 139.12, 145.60, 154.59, 156.17. MS (ES m/z): 369 (M^+-Na), 250, 121.

3-Amino-4-methyl-*N*'-(3,4-dichlorobenzylidene)thiophene-2-carbohydrazide **(2i)** Yellow solid, yield: 75%, mp: 260 °C. FT-IR: υmax (cm^{-1}): 3228 (NH), 3088 (=CH), 2960, 2929, 2872 (CH), 1666 (C=O), 1581 (C=N) 1138 (C-Cl). ^{1}H NMR (400 MHz, DMSO-d_6) δ 2.04 (3H, s, thiophene-CH3), 6.89 (1H, s, Ar-H), 7.34-7.99 (5H, m, hydrazone CH and Ar-H), 11.40 (1H, s, hydrazone NH). ^{13}C NMR (100 MHz, DMSO-d_6) δ 128.51, 130.56, 131.78, 132.33, 134.43, 134.74, 160.40.

3-Amino-*N*'-[(furan-2-yl)methylidene]-4-methylthiophene-2-carbohydrazide **(2j)** White solid, yield: 75%, mp: 120 °C. FT-IR: υmax (cm^{-1}): 3228 (NH), 3086 (=CH), 2960, 2875, 2833 (CH), 1666 (C=O), 1573 (C=N). ^{1}H NMR (400 MHz, DMSO-d_6) δ 2.09 (3H, s, thiophene-CH3), 6.63 (1H, s, Ar-H), 7.27-7.92 (5H, m, hydrazone CH and Ar-H), 11.15 (1H, s, hydrazone-NH). MS (ES m/z): 248 (M^+-H), 231, 59.

3-Amino-4-methyl-*N*'-(4-methylbenzylidene)thiophene-2-carbohydrazide **(2k)** White solid, yield: 75%, ^{1}H NMR (400 MHz, DMSO-d_6) δ 2.04 (3H, s, Ar-CH_3), 2.34 (3H, s, Ar-CH_3), 6.84 (2H, s, Ar-NH_2), 7.26-7.99 (6H, m, hydrazone CH and Ar-H), 11.16 (1H, s, hydrazone NH). ^{13}C NMR (100 MHz, DMSO-d_6) δ 13.37, 21.50, 127.36, 129.93, 132.42, 139.64. MS (ES m/z): 272 (M^+-H), 155, 59.

3-Amino-4-methyl-*N*'-(4-fluorobenzylidene)thiophene-2-carbohydrazide **(2l)** Yellow solid, yield: 70%, mp: 182 °C. FT-IR: υmax (cm^{-1}): 3259 (NH), 3066 (=CH), 2966, 2931, 2872 (CH), 1666 (C=O, amide), 1631 (C=O hydrazone), 1602(C=N), 1224 (C-F). ^{1}H NMR (400 MHz, DMSO-d_6) δ 7.35-8.73 (5H, m, hydrazone CH and Ar-H). ^{13}C NMR (100 MHz, DMSO-d_6) δ 116.48, 116.62, 131.14, 131.20, 160.89, 163.56, 165.22.

3-Amino-4-methyl-*N*'-(4-chlorobenzylidene)thiophene-2-carbohydrazide **(2m)** Yellow solid, yield: 70%, mp: 230 °C. ^{1}H NMR (400 MHz, DMSO-d_6) δ 2.04 (3H, s, thiophene-CH_3), 6.87 (2H, s, Ar-NH_2), 7.31-8.01 (6H, m, hydrazone CH and Ar-H), 11.29 (1H, s, hydrazone NH). ^{13}C NMR (100 MHz, DMSO-d_6) δ 13.37, 127.47, 128.97, 129.44, 134.08, 134.30, 156.37.

4.2. Biological Activity

4.2.1. Cell line and culture condition

The study employed MDA-MB-231 human breast cancer cells and HUVEC human umbilical vein endothelial cells. The growth and multiplication of the cells were carried out in a medium containing 10% fetal bovine serum (FBS), 1% penicillin-streptomycin, 2 mM L-glutamine, and 2000 mg/L sodium bicarbonate at 37 °C, 5% CO_2, and 75% humidity in an incubator. MDA-MB-231 cells were cultivated in DMEM medium, while HUVEC cells were grown in F12 (Kaighn's Modification of Ham's F-12 Medium) medium, supplemented with 0.04 mg/ml endothelial cell growth supplement.

4.2.2. Cell viability assay

The MTT (3-(4,5-dimethylthiazol-2-yl)-2,5-diphenyltetrazolium bromide) test was employed to ascertain the impact of the synthesized compounds on MDA-MB-231 and HUVEC cells. The IC_{50} (half-maximal inhibitory concentration) values were subsequently calculated. To this end, 5 x 10^3 MDA-MB-231 and HUVEC cells were seeded in 100 µL of medium in 96-well plates. Once the cells had adhered, the synthesized compounds were added to the cells at concentrations of 0.1, 1, 10, 100, and 1000 µM, and the

plates were incubated for 24 and 48 hours at that concentration. Following the incubation period, 10 µL of MTT solution was added to the cells (ODC Research and Development ODC0009D-250 Cytotoxicity assay kit) and incubated for four hours. The medium was then aspirated, and 100 µL of solubilization solution was added to each well to facilitate the dissolution of the formed formazan dye. The absorbance of the resulting color was then measured at 570 nm in a microplate reader. The MTT test was conducted in triplicate. The viability rate, IC_{50} calculation, and statistical analyses were then performed using the GraphPad Prism package program. Finally, images of the cells were captured under an inverted microscope at 24 hours.

4.2.3. Carbonic anhydrase inhibition analysis

Carbonic anhydrase activity measurement was performed using a commercial kit following the protocol (Abcam, ab283387). The colorimetric-based method measured CA enzyme inhibition was placed in 96 well plates, and newly synthesized compounds at 10 µM concentrations and acetazolamide (10 µM) were used. Kinetic measurement was taken at 405 nm via ELISA reader (Epoch Biotek).

4.2.4. HIF1a gene expression analysis

MDA-MB-231 cells were seeded in 6 well plates at $2x10^5$ and incubated with compounds **2b** and **2m** at 10 µM concentration for 48 hours. After incubation, the cells were collected and lysed and total RNA isolation was performed using a commercial kit (Ambion, Invitrogen). RNA concentration was measured in nanodrops and purity rates were checked. The isolated RNAs were converted to cDNA with the help of a commercial kit (Onestep cDNA synthesis kit, Applied Biosytem). Gene expression levels were examined in qPCR with SYBR green (SYBR Green master mix ABI) using specific primers (Hif1a forward primer 5′ GTCCACGTCGCCATCTTGTC'3, reverse primer 5′ CTGGGTTTTTGAGGCGGGTA'3, GAPDH forward primer 5′-TGCACCACCAACTGCTTAGC-3′, reverse primer 5′-GGCATGGACTGTGGTCATGAG-3′). The results were analyzed in ABI-Stepone Plus software using GAPDH as the housekeeping gene. Each experiment was repeated 3 times at different times by running in duplicate.

4.2.5. Measurement of HIF1a, Bax and Bcl-2 protein levels

The cells were seeded in 6-well plates and the compounds were incubated at a concentration of 10 µM for a period of 48 hours. Following the incubation period, the MDA-MB-231 cells were harvested and lysed using lysis buffer. ELISA kits (HIF-1alpha [E-EL-H6066], Human HIF1A ELISA kit; Bax [ODC00012eh], Human Bax ELISA kit; and Bcl-2 [ODC00013eh], Human Bcl-2 ELISA kit) were employed to analyze HIF-1α, Bax, and Bcl-2, respectively, according to the instructions outlined in the manufacturer's protocol. Subsequently, the samples were loaded onto the ELISA plates and washed with the wash buffer following the binding of the antibodies. Following the addition of the secondary antibody and subsequent washing step, the substrate was introduced and read at 450 nm in an ELISA reader (Epoch, Biotek). Annexin-V assay: MDA-MB-231 cells were seeded in 6-well plates at a density of 1×10^6 cells per well and incubated for 48 hours with 10 µM doses of the compounds **2b** and **2m**. Following the incubation period, the cell medium was removed and the cells were washed twice with PBS. Subsequently, the cells were detached using trypsin-EDTA and centrifuged at 500 x g for 10 minutes. The cells were prepared in accordance with the manufacturer's instructions using the Annexin-V-FITC kit (BD Pharmigen, 556570) and suspended in an annexin binding buffer. A total of 100 µL of the cell suspension was obtained, and 5 µL of both annexin V and PI were subsequently added. The mixture was then incubated for 30 minutes in the dark at room temperature. Subsequently, 20,000 cells were analyzed using a flow cytometer (Novocyte, Agilent), and the gate was selected for the examination of apoptotic cells and live cells.

4.2.6. Mitochondrial membrane potential measurement

JC-1 (5,5',6,6'-tetrachloro-1,1',3,3'-tetraethylbenzimidazolcarbocyanine iodide) is a lipophilic fluorochrome that is employed for the evaluation of the mitochondrial membrane potential (Δψ) in order to facilitate the analysis of apoptosis. MDA-MB-231 cells were seeded in 6-well plates at a density of 1×10^6 cells per well and incubated for 48 hours with 10 µM doses of the compounds **2b** and **2m**. Following the incubation period, the cell medium was removed and the cells were washed twice with PBS. Subsequently, the cells were removed with trypsin-EDTA and centrifuged at 500 x g for 10 minutes. The cells were prepared in accordance with the manufacturer's instructions using the JC-1 kit (BD Pharmingen MitoScreen (JC-1), 551302). They were suspended in PBS buffer, and 100 µL of the cell suspension was transferred to a

new tube, followed by the addition of 500 µL of the JC-1 Working Solution. The mixture was then incubated for 15 minutes in the dark at 37°C. Subsequently, the cells were subjected to centrifugation at 500 x g for 10 minutes, washed with JC-1 assay buffer, and resuspended. A total of 20,000 cells were analyzed using a flow cytometer (Novocyte, Agilent), with the gate selected and examined for JC-1 fluorescence in both the FL-1 and FL-2 channels. The red dye indicates the formation of aggregates (polarized Δψ), while the green dye indicates monomer formation (depolarized Δψ). Based on these ratios, alterations in the mitochondrial membrane were discerned.

Acknowledgements: The starting compound, Articaine, was obtained from Sanofi. We thank Sanofi for their support in materials. This research was partly supported by TÜB˙ITAK 2209-A Research Project Support Programme for Undergraduate Students (Project application no: 1919B012108418).

Author contributions: Concept – S.K., F.T., Ö.Ç.; Design – S.K., F.T., Ö.Ç.; Supervision – S.K.; Resources – S.K., F.T., B.İ.A., E.T., N.K.K., S.T., Ö.Ç.; Materials – S.K., F.T., B.İ.A., E.T., N.K.K., S.T., Ö.Ç.; Data Collection and/or Processing – S.K., F.T., B.İ.A., E.T., N.K.K., Ö.Ç.; Analysis and/or Interpretation – S.K., F.T., B.İ.A., E.T., N.K.K., Ö.Ç.; Literature Search – S.K., F.T., B.İ.A., E.T., N.K.K., S.T., Ö.Ç.; Writing – S.K., F.T., B.İ.A., E.T., N.K.K., S.T., Ö.Ç.; Critical Reviews – S.K., F.T., S.T., Ö.Ç.

Conflict of interest statement: The authors declared no conflict of interest.

REFERENCES

[1] Kashyap D, Pal D, Sharma R, Garg VK, Goel N, Koundal D, Zaguia A, Koundal S, Belay A. Global Increase in Breast Cancer Incidence: Risk Factors and Preventive Measures. Biomed Res Int. 2022; 2022: 9605439. https://doi.org/10.1155/2022/9605439.

[2] World Health Organization (WHO). International Agency for Research on Cancer (IARC). Cancer Tomorrow. Globocan 2022 (version 1.1). https://gco.iarc.who.int. (accessed on 20 July 2024).

[3] McDonald ES, Clark AS, Tchou J, Zhang P, Freedman GM. Clinical Diagnosis and Management of Breast Cancer. J Nucl Med. 2016; 57: 9S-16S. https://doi.org/10.2967/jnumed.115.157834.

[4] Akram M, Iqbal M, Daniyal M, Khan AU. Awareness and current knowledge of breast cancer. Biol Res. 2017; 50(1): 1-23. https://doi.org/10.1186/s40659-017-0140-9.

[5] Tommasi C, Balsano R, Corianò M, Pellegrino B, Saba G, Bardanzellu F, Denaro N, Ramundo M, Toma I, Fusaro A, Martella S, Aiello MM, Scartozzi M, Musolino A, Solinas C. Long-term effects of breast cancer therapy and care: calm after the storm? J Clin Med. 2022; 11(23): 1-17. https://doi.org/10.3390/jcm11237239

[6] Çakmak R, Başaran E, Şahin K, Şentürk M, Durdağı S. Synthesis of novel hydrazide–hydrazone compounds and ın vitro and ın silico ınvestigation of their biological activities against AChE, BChE, and hCA I and II. ACS Omega. 2024;9(18): 20030–20041. https://doi.org/10.1021/acsomega.3c10182

[7] Tok F, Çelikçi T, Acar AB, Baltaş N, Başoğlu F, Karakuş S. Synthesis, in-vitro inhibition of cholinesterase and in silico studies of new hydrazide-hydrazones derived from Clopidogrel. J Mol Struct. 2024; 1314: 138763. https://doi.org/10.1016/j.molstruc.2024.138763

[8] Tok F, Sağlık BN, Özkay Y, Kaplancıklı ZA, Koçyiğit-Kaymakçıoğlu B. Design, synthesis, biological activity evaluation and in silico studies of new nicotinohydrazide derivatives as multi-targeted inhibitors for Alzheimer's disease. J Mol Struct. 2022; 1265: 133441. https://doi.org/10.1016/j.molstruc.2022.133441

[9] Tok F, Sağlık BN, Özkay Y, Kaplancıklı ZA, Koçyiğit-Kaymakçıoğlu B. N-substituted arylidene-3-(methylsulfonyl)-2-oxoimidazolidine-1-carbohydrazide as cholinesterase ınhibitors: Design, synthesis, and molecular docking study. Chem Biodivers. 2022; 19(8): e202200265. https://doi.org/10.1002/cbdv.202200265

[10] Akdağ K, Ünal G, Tok F, Arıcıoğlu F, Temel HE, Koçyiğit-Kaymakçıoğlu B. Synthesis and biological evaluation of some new hydrazone derivatives bearing pyrimidine ring as analgesic and anti-inflammatory agents. Acta Pol Pharm. 2018; 75(5): 1147-1159. https://doi.org/10.32383/appdr/86743

[11] Murugappan S, Dastari S, Jungare K, Barve NM, Shankaraiah N. Hydrazide-hydrazone/hydrazone as enabling linkers in anti-cancer drug discovery: A comprehensive review. J Mol Struct. 2024; 1307: 138012. https://doi.org/10.1016/j.molstruc.2024.138012

[12] Acar Çevik U, Sağlık BN, Ardıç CM, Özkay Y, Atlı Ö. Synthesis and evaluation of new benzimidazole derivatives with hydrazone moiety as anticancer agents. Turk J Biochem. 2018; 43(2): 2018, 151-158. https://doi.org/10.1515/tjb-2017-0167

[13] Osmaniye D, Levent S, Karaduman AB, Ilgın S, Özkay Y, Kaplancıklı ZA. Synthesis of new benzothiazole acylhydrazones as anticancer agents. Molecules. 2018; 23(5): 1054. https://doi.org/10.3390/molecules23051054

[14] Akdağ K, Tok F, Karakuş S, Erdoğan Ö, Çevik Ö, Koçyiğit-Kaymakçıoğlu B. Synthesis and biological evaluation of some hydrazide-hydrazone derivatives as anticancer agents. Acta Chim Slov. 2022; 69: 863-875. https://doi.org/10.17344/acsi.2022.7614

[15] Saral Çakmak S, Erdoğan Ö, Başoğlu F, Çoruh U, Çevik Ö, Karakuş S. Exploring etofenamate hydrazide-hydrazone/copper(II) complexes: Synthesis, anticancer activity, carbonic anhydrase IX inhibition and docking studies. J Mol Struct. 2024; 1312: 138555. https://doi.org/10.1016/j.molstruc.2024.138555

[16] Koçyiğit-Kaymakçıoğlu B, Yazıcı SS, Tok F, Dikmen M, Engür S, Oruç Emre EE, İyidoğan A. Synthesis and anticancer activity of new hydrazide-hydrazones and their Pd(II) complexes. Lett Drug Des Discov. 2019; 16(5): 522-532. https://doi.org/10.2174/1570180815666180816124102

[17] Li Y, Wang H, Oosterwijk E, Tu C, Shiverick KT, Silverman DN, Frost SC. Expression and activity of carbonic anhydrase IX ıs associated with metabolic dysfunction in MDA-MB-231 breast cancer cells. Cancer Invest. 2009; *27*(6): 613–623. https://doi.org/10.1080/07357900802653464

[18] Potter C, Harris AL. Hypoxia inducible carbonic anhydrase IX, marker of tumour hypoxia, survival pathway and therapy target. Cell Cycle. 2004; 3(2): 164-167.

[19] Simko V, Takacova M, Debreova M, Laposova K, Ondriskova-Panisova E, Pastorekova S, Csaderova L and Pastorek J. Dexamethasone downregulates expression of carbonic anhydrase IX via HIF-1α and NF-κB-dependent mechanisms. Int J Oncol. 2016; 49: 1277-1288. https://doi.org/10.3892/ijo.2016.362